

RESEARCH COMMUNICATION

The structure of the quinoprotein alcohol dehydrogenase of *Acetobacter aceti* modelled on that of methanol dehydrogenase from *Methylobacterium extorquens*

Gyles Eldred COZIER, Ian G. GILES and Christopher ANTHONY*

SERC Centre for Molecular Recognition, Department of Biochemistry, University of Southampton, Southampton SO16 7PX, U.K.

The 1.94 Å structure of methanol dehydrogenase has been used to provide a model structure for part of a membrane quinohaemoprotein alcohol dehydrogenase. The basic superbarrel structure and the active-site region are retained, indicating

essentially similar mechanisms of action, but there are considerable differences in the external loops, particularly those involved in formation of the shallow funnel leading to the active site.

INTRODUCTION

The term quinoprotein was first coined by Duine and Frank [1] to include dehydrogenases that contain as their prosthetic group pyrroloquinoline quinone (PQQ). This group of NAD(P)-independent enzymes includes methanol dehydrogenase (MDH) of methylotrophic bacteria [2–4] and the quinohaemoprotein alcohol dehydrogenase (ADH) from acetic acid bacteria [5]. MDH is a soluble periplasmic enzyme, having cytochrome c_1 as electron acceptor [6]. By contrast, in ADH electrons pass from PQQH₂ to a haem c on the same quinohaemoprotein subunit, and thence to ubiquinone in the membrane by way of a separate cytochrome c subunit in the three-component membrane complex [7].

MDH is the only PQQ-containing quinoprotein for which an X-ray structure is available, and it is the recent high-resolution structure of the enzyme from *Methylobacterium extorquens* [4,8] that is used for the basis of the present paper. MDH has an $\alpha_2\beta_2$ tetrameric structure, each α subunit (66 kDa) having a single molecule of PQQ and a Ca²⁺ ion. The small β -subunits (8.5 kDa) fold around the surface of the α -subunits. The α -subunit is a superbarrel made up of eight topologically identical four-stranded antiparallel β -sheets (W-shaped) arranged with radial symmetry like the blades of a propeller. The PQQ is buried in the interior of the superbarrel within a chamber that communicates with the exterior through a hydrophobic funnel-shaped depression in the surface. The floor of the active-site chamber is formed by the plane of a tryptophan residue, the ceiling being formed by a novel ring structure arising from a disulphide bridge between adjacent cysteine residues. A second important feature seen in the active site is a Ca²⁺ ion, which plays a role in maintaining PQQ in the correct configuration and which may also be involved in the catalytic mechanism.

The quinohaemoprotein subunit of the membrane ADH complex is larger than MDH, having a C-terminal extension of residues that includes the haem c site [9,10]. The N-terminal region of ADH (about 600 residues) and the α subunit of MDH (total 599 residues) show sufficient identity of sequence (31%) to indicate that they might have essentially the same type of

superbarrel structure. Although Ca²⁺ has never been shown to be present in this ADH, because it oxidizes primary alcohols (excluding methanol), it might be expected to have a similar mechanism and thus to bind Ca²⁺ at its active site near PQQ, as shown for MDH.

This paper presents the results of modelling the sequence of the N-terminal region of subunit I of the quinohaemoprotein ADH on to the co-ordinates of the α subunit of MDH in an attempt to identify regions of structure that might be responsible for their different activities.

METHODS

The sequences of the α and β subunits of MDH were those for the enzyme from *Methylobacterium extorquens* [11–13]. The primary sequence of the ADH is that of the α subunit (the quinohaemoprotein unit, sometimes called subunit I) of the quinohaemoprotein-cytochrome c ADH dehydrogenase membrane complex of *Acetobacter aceti* [9,10,13]. Alignment and modelling were conducted by using residues 1–595 of MDH and 1–590 of ADH (Figure 1); residues 591–707 of ADH constitute an additional domain in which the haem-binding site is thought to be located. In the regions selected there was a 31% identity and 66% similarity of sequence. All analysis and modelling were performed with the program package Quanta/CHARMm. Sequence alignment was initially determined by using a Needleman–Wunsch algorithm [14] and a protein-sequence score matrix [15]. This alignment was then refined by hand where necessary, assuming conservation of residues known to be structurally significant in the β -sheet superbarrel of MDH. Wherever possible, inserts or deletions were incorporated opposite the loop regions of MDH rather than in the β -sheet 'W' motifs. The backbone co-ordinates of aligned residues in MDH were then mapped to the equivalent amino acids in ADH. Where inserts or deletions occurred in ADH, a fragment database [16] was used to search for short sequences that overlapped with the structure on either side of the unknown region and that contained

```

MDH 1-      NDKLVELSKSDNWMVPGKNYDSNNFSDLKQINKCNVKQLRP AWTFFSTGL
ADH 1-DGQGTGEAIIHADDHPENWLSYGRITYSEQRYSPLDQINRSVNGDLKLLGYTLDT

MDH 51-LNGHEGAPLVVDGKMIHTSFPNNTFALGLDDPGTILWQDKPKQNPAAARAVACCDL
ADH 57-NRQGQEATPLVVDGIMYATTN-SKMEALD-AATGKLLWQYDKVPNGTAADKGGCCDT

MDH 107-VNRGLAYWPGDGKTPALI LKTQLDGNVAALNAETGETVWKVEN-----S--DIKVG
ADH 111-VNRGAGYW--NG-----KVFWGTEDGRLVAADAKTKKKVAVNTIIPADASLGKQ--R

MDH 156-S-TLTIAPYVVKDKVIIGSSGAELGVRGYLTAYDVKTGEQVWRAYATGPD--KDLL
ADH 159-SYTVDGAVRVAKGLVLI GNNGGAEGARGFVSAFDAETGKLRWFYTPVNNKNE-PD

MDH 209-L-ASDFNIKNPHYGQKGLGTCTWEGDAWKIGGCTNWCWYAYDPCTNLIYFCGTGSPA
ADH 214-HAASDNILMNAKAYKTWG-PKG---AWVRQGGGGTVWDSLVYDVPVSDLIYLA VGNNGS

MDH 264-PWNE-TMR--PGDNKWTMTIFGRDADTGEAKFGYQKTPHDEWDYAGVNVNMLSEQK
ADH 266-PWNYKYRSEGISNLFGLSIVALKPETGEYVWHFQATPMQWDYTSVQQIMTLDMF

MDH 317-DKDGKARKLLTHPDRNGIYVYTLDRDTGALVLSANKLDDTVNVFKSVDLKTGQPVYRDP
ADH 322-VK-GERMHVIVHAPKNGFFYLDARTGEFLSGKNYVYQNA-NGLDPLTRGPMYD

MDH 373-EYGTMRDHLAKDICPSAMGYHNQGHSDYDKRELFMGINHICMDWEPFMLPYR--
ADH 376-DGLYTLNGKFWYGI PGPLGAHNFAMAYSPKTHLVYI PAHQIPFGYKNQVGGFKPH

MDH 427-AQGFVFGATLNM--YPCPKGDRQNY--EGLGQIKAYNAITGDYKWEKMERFAVW-G
ADH 432-ADSNVGLDMTKNGLPDTPEARAYIKDLHGWLAWDPVKMETVWKID-HKGPWNG

MDH 478-GTMTAGDLVFFYCTLDGYLKARDSDTCDLLWKFIPSGAIGYPMYTHKGTQYVAI
ADH 487-GILATGDDLFGQLANGEFHAYDATNGSDLYKFDQSGI IAPPMTYSVNGKQYVAV

MDH 534-YYGVGGWPGVGLVFDLADPTAGLGAVGAFKKLANYTQMGGGVVVFLDGKGPYDDP
ADH 543-EVGGGGYI-----PISMGV---GRTSGWTVNHSYIAAFSLDGKAKLPAL

MDH 590-NVGEWK -595
ADH 585-NNRGFL -590

```

Figure 1 Alignment of the amino acid sequences of MDH and ADH

the same number of residues. The best-fit fragment was then used to model the ADH. After defining the backbone co-ordinates, the validity of the emerging structure was assessed by using the Protein Health module in Quanta. The irregularities identified were either remodelled manually or by re-using the fragment database. Once the backbone residues had been defined, the side-chain co-ordinates of the identical amino acids were also copied from MDH to ADH. Quanta/CHARMm was then used to generate side chains for the non-identical amino acids in their most likely rotameric form. Major side-chain clashes were removed manually, and then CHARMm was used to perform an energy minimization, applying constraints to preserve the basic backbone structure as in MDH. As the energy minimization is based on absolute zero, and the MDH structure was determined at about 20 °C, the MDH structure was also minimized by using similar constraints to those used to model the ADH. The final energies obtained were of the same order of magnitude, and the MDH did not show major structural perturbations during minimization. The final structure was checked for abnormalities and inconsistencies by using the Protein Health option in Quanta.

RESULTS AND DISCUSSION

The superbarrel structure

The overall structure of the model ADH is compared with the structure of MDH in Figure 2. The regions of greatest sequence similarity are the eight β -sheet regions (the 'W' motifs or propeller blades), and these sequences in ADH model very well on to the MDH structure. These β -sheet 'W' motifs are held together by special tryptophan docking motifs made up of 11-residue consensus sequences. These form a planar stabilizing girdle of interactions around the periphery of the subunit [8]. Figure 3 shows the 11-residue consensus sequences that form the docking motifs, and Figure 4 shows a typical docking motif in ADH. The only difference in the consensus sequences of the two proteins is that the carboxylate at position 8 in MDH is replaced by lysine in ADH.

Before the structure of MDH had been determined, it had been suggested that a region showing the greatest sequence identity in quinoproteins (50%) might represent a PQQ-binding domain (residues 477–539 in MDH, 486–548 in ADH; 50%

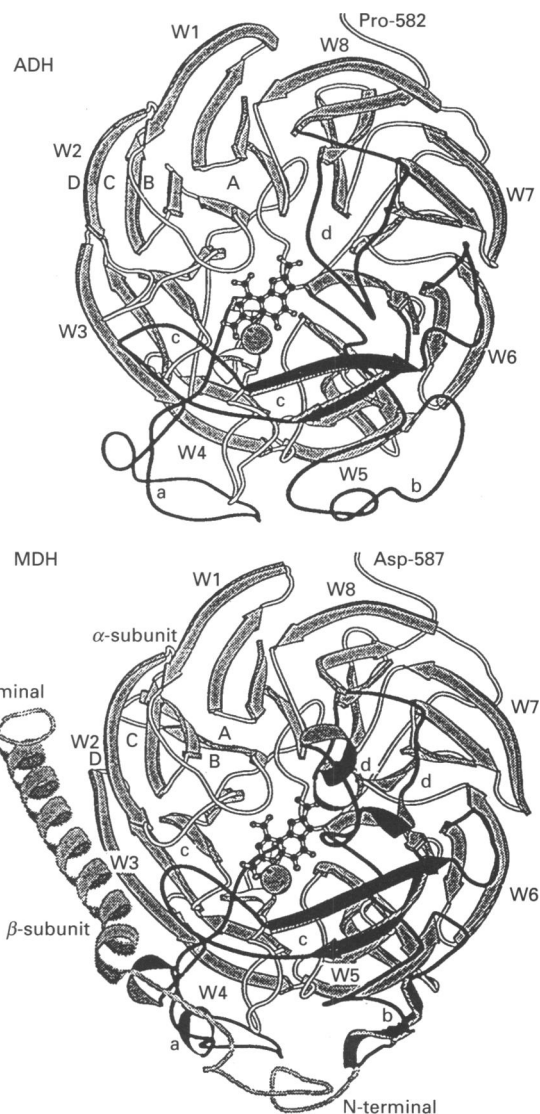


Figure 2 Schematic representation of the backbone of ADH (a) and MDH (b), showing their major secondary structural features

The model ADH structure is of part of the quinohaemoprotein subunit of the membrane complex; the MDH is the structure previously published for the α and β subunits, which form an $\alpha_2\beta_2$ tetramer [4,8]. The prosthetic group is shown as a ball-and-stick structure, and the Ca^{2+} as a van der Waal's sphere. The major loops (in black) are: (a) residues 205–245 (ADH) and 201–243 (MDH); (b) 356–389 (ADH) and 352–386 (MDH); (c) 418–460 (ADH) and 415–451 (MDH); (d) 546–565 (ADH) and 537–570 (MDH). The Figure was generated with Molscript [17].

identity) [4,9,13]. However, the reason for this higher degree of identity is not obvious, because this sequence constitutes the whole W7 motif plus the A and B strands of W8, which are almost identical in MDH and ADH, but are not involved in the active site.

Two of the three *cis* proline residues of MDH are conserved in ADH. Pro-72 is replaced by Ser-78, but this has no major effect, because Pro-72 occurs on a β -turn which is retained in ADH. Besides the novel disulphide bridge between adjacent cysteines, there is only one other disulphide bridge in MDH (Cys-386–Cys-415) and this is not conserved in ADH, which therefore contrasts with MDH in having no disulphide bridge connecting the two

Position	1	2	3	4	5	6	7	8	9	10	11
W1	Ala 82	Leu	Asp	Ala	Ala	Thr	Gly	Lys	Leu	Leu	Trp 92
W2	Ala 133	Ala	Asp	Ala	Lys	Thr	Gly	Lys	Lys	Val	Trp 143
W3	Ala 190	Phe	Asp	Ala	Glu	Thr	Gly	Lys	Leu	Lys	Trp 200
W4	Ala 287	Leu	Lys	Pro	Glu	Thr	Gly	Glu	Tyr	Val	Trp 297
W5	Val 341	Leu	Asp	Ala	Lys	Thr	Gly	Glu	Phe	Leu	Ser 351
W6	Ala 466	Trp	Asp	Pro	Val	Lys	Met	Glu	Thr	Val	Trp 476
W7	Ala 507	Tyr	Asp	Ala	Thr	Asn	Gly	Ser	Asp	Leu	Tyr 517
W8	Ala 572	Phe	Ser	Leu	Asp 576	Asp 45	Leu	Lys	Leu	Leu	Gly 50
ADH Consensus	Ala	X	Asp	Ala	X	Thr	Gly	Lys/Glu	X	Leu/Val	Trp
MDH Consensus	Ala	X	Asp/Asn	X	X	Thr	Gly	Asp/Glu	X	X	Trp

Figure 3 Consensus sequences in the tryptophan docking motifs in the model ADH

This docking occurs at the C-D corners at the end of the C strands and the beginning of the D strands of each 'W' motif; there are no loops between these strands. The consensus sequence for MDH is included (from [8]). Consensus residues are indicated in **bold** type. The tryptophan in position 11 forms stacking interactions between alanine (position 1) on the same motif and the peptide bond between positions 6 and 7 on the following motif (see Figure 4). This interaction was first described for MDH by F. Scott Mathews in the 3rd Symposium on PQQ and Quinoproteins (Capri, 1994) and has been described in full in reference [8].

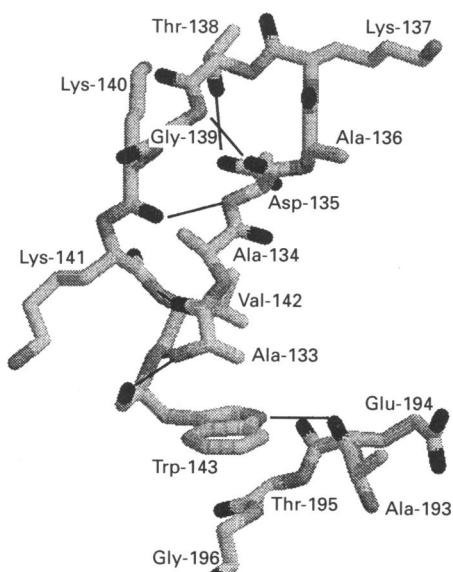


Figure 4 A typical tryptophan docking motif in the model ADH

This shows Trp-143 in a stacking interaction between Ala-133 and the peptide bond between Thr-195 and Gly-196. There is also a hydrogen bond between the indole of Trp-143 and the peptide carbonyl group of Ala-193. For clarity, the side chain of Thr-195 is not included.

large exterior loops (residues 356–389 and 418–460 in ADH; 352–386 and 415–451 in MDH) (Figure 2).

Although there are six extra residues in ADH at the N-terminus, the subsequent 40 residues up to the start of the first β -sheet motif show 30% identity and can be modelled to give the same random coil that forms a base to the superbarrel in MDH. The regions where the two proteins differ most are in the loop regions between the B and C strands within the β -sheet W motifs, and between the D and A strands of adjacent motifs (Figure 2). These regions are discussed in the context of their functions below.

The loops on the sides of the superbarrel

The first part of loop 205–245 (201–243 in MDH) shows some sequence identity, but MDH has some helical structure, which is absent in ADH (Figure 2). The only markedly similar part of this region is immediately before Trp-245, which forms the floor of the active-site chamber and which includes Thr-243 (Thr-241 in MDH), which co-ordinates to the 7-carboxylate of PQQ. The second of these loops (356–389 in ADH, 352–386 in MDH) in the model ADH differs from MDH in order to accommodate the higher number of aromatic residues on this loop and also on the neighbouring D strand of W5.

The intersubunit interactions in MDH

The α subunits of MDH interact with each other over a large planar interface involving hydrophobic and hydrophilic side

chain interactions of the D strands of W7 and W8 and the last 10 C-terminal residues [8]. The residues involved in hydrophobic stacking interactions in MDH (Pro-42/Pro-42 and Leu-51/Leu-51) are not conserved in ADH, nor are most of the residues involved in hydrophilic interactions. This is consistent with some evidence that the membrane complex consists of only one subunit of each of its three component proteins [5].

ADH has not been reported to have a small β -subunit equivalent to that in MDH (8.5 kDa). In MDH the β -chain runs across the surface of the α -subunit, making contact all along its length with the edges of the W1–W4 motifs by way of ion-pair interactions involving Glu-148, Glu-193, Arg-197, Lys-236, Glu-267 and Glu-301. In the ADH model only two of these (the equivalents of Glu-193 and Glu-197) could be involved in ionic interactions, consistent with the observed lack of an equivalent β -subunit in ADH [5]. No convincing specific role for the unusual non-globular β -subunit in MDH has been proposed, except that it might act to stabilize the folded form of the large α -chain [4,8]. If this is the case, then perhaps a similar stabilizing role in ADH is provided by its interaction with the other components of the membrane complex.

The active-site funnel in the surface

A remarkable feature of the surface of MDH is the shallow hydrophobic funnel that leads to the active site [4]. It involves three separate loop regions and consists of the following residues (surface-accessible residues in MDH in **bold type**):

MDH: 100-**AVACCDL**; 420-**PFMLP**; 430-**FFV**; 540-**WPGVGLVFDLADPTAGL**-
 ADH: 104-DKGCCDT; 423-NQVGG; 435-WNV; 549-IY-----PISM

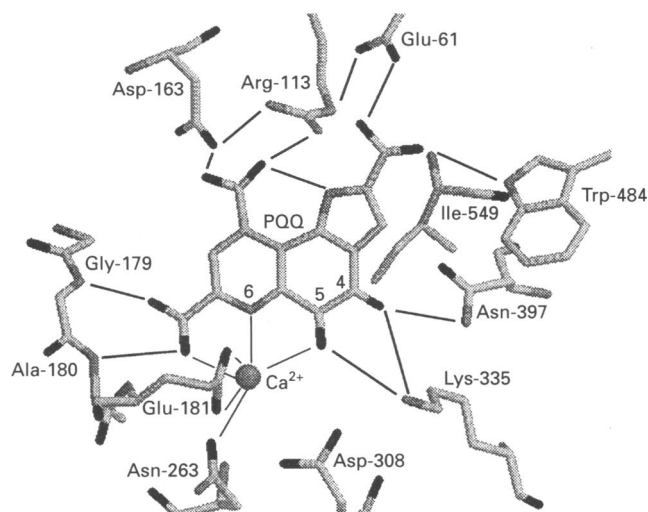


Figure 5 The co-ordination of Ca^{2+} and bonding of PQQ at the active site of the model ADH

In addition to these equatorial interactions, PQQ is 'sandwiched' between the indole ring of Trp-245 and the two sulphur atoms of the novel disulphide ring made up of Cys-107/Cys-108. By analogy with the mechanism proposed for MDH [4], Asp-308 acts as a base, initiating the reaction by abstracting a proton from ethanol; in this mechanism the Ca^{2+} acts as a Lewis acid, co-ordinating with the C-5 carbonyl oxygen, which gives rise to the electrophilic C-5 carbon of PQQ. The most significant difference in this model active site of ADH and that of MDH is that Arg-331 in MDH is replaced in ADH by Lys-335.

A small loop between D1 and A2 includes the adjacent cysteines (103–104) which make up the novel disulphide ring at the base of the funnel leading into the active site. The second loop (415–450 in MDH, 418–459 in ADH) has little sequence identity and includes six extra residues in ADH, but it has a similar hairpin β -structure in the model ADH and forms part of the funnel in both proteins. The third loop (537–570 in MDH, 546–565 in ADH) has negligible sequence similarity and is much smaller in ADH, which lacks the helical structure seen in MDH (Figure 2).

This surface funnel region shows the greatest difference between the two proteins, mainly due to the absence in ADH of the hydrophobic helical structure that is so prominent in MDH. This is the part of the surface nearest to the prosthetic group and is an obvious region for interaction with the electron acceptor cytochrome c_L . By contrast with MDH, one side of the funnel in ADH is rather polar and may be involved in interaction with its C-terminal region containing the haem that has been proposed to be the electron acceptor from the quinol prosthetic group in this protein.

The active site

In MDH and the model ADH the PQQ ring is sandwiched between the indole ring of a tryptophan (Trp-243 in MDH, Trp-245 in ADH) and the two sulphur atoms of the novel disulphide-ring structure. In addition to this, there are many equatorial interactions between substituent groups of the PQQ ring system

and amino acid residues, mainly on the A strands of the β -sheets of the superbarrel. These residues in ADH are Glu-61, Arg-113, Asp-163 (Thr-159 in MDH), Gly-179, Ala-180, Thr-243, Lys-335 (Arg-331 in MDH), Asn-397, Trp-484 and Ile-549 (Trp-540 in MDH) (Figure 5). Where there are differences in the two proteins, they form similar interactions with the PQQ, an exception being Ser-174 in MDH, which is replaced by Gly-178 in ADH and thus unable to interact with the 9-carboxylate group of PQQ.

In MDH the co-ordination sphere of the Ca^{2+} in the active site contains PQQ atoms, both oxygens of the carboxylate group of Glu-177, and the amide oxygen of Asn-261. The PQQ donor atoms include the C-5 quinone oxygen, one oxygen of the C-7 carboxylate group and, remarkably, the N-6 ring atom. In the active site of the model ADH, the nature and position of all these residues are conserved, strongly indicating that Ca^{2+} fulfils a similar role in the two enzymes. It has been suggested that the Ca^{2+} ion might act as a Lewis acid, through its co-ordination with the C-5 carbonyl oxygen, thus providing the electrophilic C-5 for attack by an oxyanion or hydride from the substrate. In this way the Ca^{2+} could play a dual role in structure and catalysis. Figure 5 shows that Asp-308 occupies the same position in the model ADH as Asp-303 occupies in MDH. This is of importance, because it has been suggested that it has the role of an active-site base, initiating reaction with the alcohol substrate by proton abstraction [3,4,8].

We thank Minakshi Ghosh for valuable discussions, and for financial support we thank the SERC and The Wellcome Trust.

REFERENCES

- 1 Duine, J. A., Frank, J. and van Zeeland, J. K. (1979) *FEBS Lett.* **108**, 443–446
- 2 Anthony, C. (1986) *Adv. Microb. Physiol.* **27**, 113–210
- 3 Anthony, C. (1993) in *Principles and Applications of Quinoproteins* (Davidson, V. L., ed.), pp. 17–45, Marcel Dekker New York
- 4 Anthony, C., Ghosh, M. and Blake, C. C. F. (1994) *Biochem. J.* **304**, 665–674
- 5 Tamaki, T., Fukaya, M., Takemura, H., Tayama, K., Okumura, H., Kawamura, Y., Nishiyama, M., Horinouchi, S. and Beppu, T. (1991) *Biochim. Biophys. Acta* **1088**, 292–300
- 6 Anthony, C. (1992) *Biochim. Biophys. Acta* **1099**, 1–15
- 7 Matsushita, K., Toyama, H. and Adachi, O. (1994) *Adv. Microb. Physiol.* **36**, 247–301
- 8 Ghosh, M., Anthony, C., Harlos, K., Goodwin, M. G. and Blake, C. C. F. (1995) *Structure* **3**, 177–187
- 9 Inoue, T., Sunagawa, M., Mori, A., Imai, C., Fukuda, M., Takagi, M. and Yano, K. (1990) *J. Ferment. Bioeng.* **70**, 58–60
- 10 Inoue, T., Sunagawa, M., Mori, A., Imai, C., Fukuda, M., Takagi, M. and Yano, K. (1989) *J. Bacteriol.* **171**, 3115–3122
- 11 Anderson, D. J., Morris, C. J., Nunn, D. N., Anthony, C. and Lidstrom, M. E. (1990) *Gene* **90**, 173–176
- 12 Nunn, D. N., Day, D. J. and Anthony, C. (1989) *Biochem. J.* **260**, 857–862
- 13 Anthony, C. (1992) *Int. J. Biochem.* **24**, 29–39
- 14 Needleman, S. B. and Wunsch, C. D. (1970) *J. Mol. Biol.* **48**, 443–453
- 15 Dayhoff, M. D. (1978) *Atlas of Protein Sequences and Structure*, Volume 5, Suppl. 3
- 16 Bernstein, F. C., Koetzle, T. F., Williams, G. J. B., Meyer, E. F., Brice, M. D., Rogers, J. R., Kennard, O., Shimanouchi, T. and Tasumi, M. (1977) *J. Mol. Biol.* **112**, 535–542
- 17 Kraulis, P. J. (1991) *J. Appl. Crystallogr.* **24**, 946–950

Received 20 February 1995/9 March 1995; accepted 13 March 1995